Retinal Layer Thicknesses in Early Age-Related Macular Degeneration: Results From the German AugUR Study

Caroline Brandl,[1–3] Christiane Brücklmayer,[1] Felix Günther,[1,4] Martina E. Zimmermann,[1] Helmut Küchenhoff,[4] Horst Helbig,[2] Bernhard H. F. Weber,[3] Iris M. Heid,[1] and Klaus J. Stark[1]

[1]Department of Genetic Epidemiology, University of Regensburg, Regensburg, Germany
[2]Department of Ophthalmology, University Hospital Regensburg, Regensburg, Germany
[3]Institute of Human Genetics, University of Regensburg, Regensburg, Germany
[4]Statistical Consulting Unit StaBLab, Department of Statistics, Ludwig-Maximilians-University Munich, Germany

PURPOSE. To systematically analyze thicknesses of retinal layers in an older population and their link to early age-related macular degeneration (AMD).

METHODS. In the AugUR baseline survey from a population aged ≥70 years, we conducted multimodal retinal imaging, including spectral-domain optical coherence tomography. Autosegmentation of eight distinct retinal layers was followed by manual correction of segmentation errors. AMD status was graded on color fundus images according to the Three Continent AMD Consortium Severity Scale. We tested the association of early AMD on retinal layer thicknesses by using linear mixed models and replicated significant results in independent data also from the AugUR platform.

RESULTS. When comparing layer thicknesses between early AMD and no AMD (822 eyes, 449 participants), the retinal pigment epithelium/Bruch's membrane complex demonstrated a statistically significant thickening (e.g., $P = 6.41 \times 10^{-92}$ for severe early versus no AMD) and photoreceptor layers showed a significant thinning. Autosegmented retinal layer thicknesses revealed similar associations as manually corrected values but underestimated some effects. Independent replication analysis in 1026 eyes (546 participants) confirmed associations (e.g., $P = 9.38 \times 10^{-36}$ for retinal pigment epithelium/Bruch's membrane complex, severe early versus no AMD).

CONCLUSIONS. This first population-based study on spectral-domain optical coherence tomography-derived retinal layer thicknesses in a total of ∼1000 individuals provides insights into the reliability of autosegmentation and layer-specific reference values for an older population. Our findings show a difference in thicknesses between early AMD and no AMD for some retinal layers, suggesting these as potential imaging biomarkers. The thinning of photoreceptor layers substantiates a photoreceptor cell loss/damage already occurring in early AMD.

Keywords: age-related macular degeneration (AMD), optical coherence tomography (OCT), population-based study of the elderly, retinal layer segmentation, retinal layer thicknesses, imaging biomarker

Age-related macular degeneration (AMD) represents the leading cause of central vision loss in the older population of industrialized countries. This degenerative disorder affects the choroid/Bruch's membrane (BrM)/retinal pigment epithelium (RPE)/photoreceptor complex of the central retina.[1,2] AMD-associated lesions can be classified into early and late disease stages via funduscopy or via color fundus photography, the latter being the gold standard for standardized and repeatable assessment in epidemiologic studies. Early AMD is determined by differently sized yellowish accumulations of extracellular material between BrM and RPE (drusen), or between RPE and the photoreceptors (subretinal drusenoid deposits).[3–5] Other features of early AMD are RPE abnormalities, including depigmentation or increased pigmentation.[2,5] Late AMD can either appear as a neovascular (NV) complication characterized by choroidal/subretinal ingrowth of diseased blood vessels, bleeding and scaring, or an atrophic form known as geographic atrophy (GA) of the RPE.[2,5]

In addition to funduscopy and en face color fundus images, other imaging modalities, particularly spectral-domain optical coherence tomography (SD-OCT) with its extremely high axial resolution of the retina (typically 3–8 μm) allow for unprecedented in vivo studies of the macula.[6,7] These have become clinically routine to diagnose and guide treatment for various retinal diseases, including AMD.[2,5,7,8] SD-OCT has been shown to reveal qualitative and quantitative imaging biomarkers linked to early AMD stages that are not readily appreciated on funduscopy and/or color fundus imaging.[5,9,10]

While the measurement of overall retinal thickness via SD-OCT has long been established,[11] recently introduced commercial, automated segmentation software now enables a systematic quantitative analysis of single retinal layers and their thicknesses by delineating optical reflectivity boundaries.[7,12–18]

These software approaches currently enable the segmentation and quantification of most, but not all, retinal layers/zones as defined by the International Nomenclature for Optical Coherence Tomography Panel.[19] The automated retinal layer segmentation has been applied in some studies with relatively small sample sizes to obtain quantitative data on AMD. For example, Muftuoglu et al.[7] analyzed 90 eyes from 60 patients with early AMD and 30 healthy controls recruited from an US eye clinic to investigate inner retinal layers and found that the inner plexiform layer (IPL) becomes thinned as the severity of early AMD increases. Another larger evaluation of 269 subjects with advanced early AMD versus 115 older subjects without AMD from the Age-Related Eye Disease Study 2 Ancillary SD-OCT Study focused on the RPE layer and found it to distinguish advanced early AMD from normal eyes.[6] However, there has not yet been any analysis encompassing each of the single retinal layers provided by segmentation software in a population-based study and their association with AMD. Furthermore, the reliability of automated retinal layer segmentation procedures has been questioned, for example by Muftuoglu et al.[7] reporting 90% of eyes to require manual correction after autosegmentation.

We have, thus, set out to establish population-based quantitative SD-OCT data in a total of nearly 1000 individuals aged 70 to 95 years from the German AugUR study platform (Age-related diseases: understanding genetic and nongenetic influences—a study at the University of Regensburg), a prospective study from the general older population.[20] In AugUR, we have recently estimated early and late AMD prevalence by using color fundus images.[21] In the present analysis, we determined thicknesses of each retinal layer given by the Spectralis SD-OCT (Heidelberg Engineering, Heidelberg, Germany) to investigate the reliability of autosegmentation via comparison to manually corrected data and to provide reference values in an older population. Moreover, we aimed to test association of early AMD with each retinal layer thickness in our cross-sectional study data to pinpoint candidates for quantitative imaging biomarkers.

SUBJECTS AND METHODS

Study Population and Study Sample

AugUR is a research platform recruiting from the general mobile population aged ≥70 years, for which we here present results from the first baseline survey conducted in 2013 to 2015. The study protocol and recruitment procedures have been described previously.[20,21] Briefly, inhabitants of the city and county of Regensburg, Germany, of ≥70 years of age, were identified by local registries and invited to the study center at the Regensburg University Hospital. Individuals were included into the AugUR study if they were able and willing to come to the study center, to participate in a three-hour study program, and to provide informed written consent. By this recruiting strategy, our study sample is drawn from a mobile population aged 70+ from Bavaria, including urban and rural areas.

The study protocol was approved by the Ethics Committee of the University of Regensburg, Germany (vote 12-101-0258). The study complies with the 1964 Declaration of Helsinki and its later amendments.

Among the 1133 individuals included in the AugUR baseline survey from 2013 to 2015, all participants from 2014 to 2015 were included into the AugUR OCT substudy and received SD-OCT imaging. This accounted to 510 randomly selected participants with acquired SD-OCT images for at least one eye.

Assessment and Segmentation of SD-OCT Images

Macular cube volumetric SD-OCT scans with 49 Raster lines, 20 × 20°, interscan distance of 120 μm between the 49 B-scans, 30 automated real-time repetitions, centered on the fovea, were acquired after mild mydriasis[20,21] via the Spectralis SD-OCT Plus BluePeak platform (Heidelberg Engineering) and imported into the Heidelberg Eye Explorer software, version 1.9.17.0 (Heidelberg Engineering).

The built-in feature for automated segmentation of retinal layers was applied, followed by manual inspection for obvious segmentation errors (i.e., improper delineations of optical reflectivity boundaries and their representative lines in any portion of at least one of the 49 cross-sectional images), and/or mislocalization of the cube (i.e., not correctly centered on the fovea). Mislocalized scans were either manually repositioned on the fovea or excluded from analysis, if the foveal region was not captured by the macular cube impeding correct positioning. Eyes were moreover excluded in the case of low-quality scans or severe retinal pathologies that made the scans ineligible for manually distinguishing retinal layers.

If required, manual adjustment of retinal layers, supported by built-in software tools, was conducted by a trained grader (ChB, supervised by senior ophthalmologist CB) paying close attention to the reflectivity of each layer. If the software was not able to draw the borders of a layer, boundary lines were manually drawn using the software's caliper function. All required manual corrections were documented (which layers, which Raster lines). Scans were excluded from analysis if distinguishing reflectivity boundaries, and thus manual corrections, were impossible due to low image quality or severe pathologic retinal alterations.

The Heidelberg Eye Explorer software output includes mean retinal layer thickness values from nine macular subfields determined by the Early Treatment Diabetic Retinopathy Study (ETDRS) grid. Using the exported data, we combined nasal, temporal, superior, and inferior subfields of the grid as described in previous reports[22,23] and analyzed mean retinal layer thicknesses in the central, inner, and outer macular circles (1, 3, and 6 mm diameter, respectively). The software provides thickness values and nomenclature of seven distinct layers: (1) the retinal nerve fiber layer (RNFL), (2) the ganglion cell layer (GCL), (3) the IPL, (4) inner nuclear layer (INL), (5) the outer plexiform layer (OPL), (6) outer nuclear layer (ONL), and (7) the RPE.

Additionally, three combinations of layers are measured and given by the software: the combined inner retinal layers (IRL, ranging from inner limiting membrane to external limiting membrane), the outer retinal layers (ORL, ranging from external limiting membrane to BrM), and the overall retinal thickness, ranging from inner limiting membrane to BrM.

As this nomenclature of retinal layers given by the Heidelberg Eye Explorer software output is not fully consistent with the consensus nomenclature developed by the International Nomenclature for Optical Coherence Tomography Panel,[19] we provide a table to compare terminology, to avoid misinterpretation (Supplementary Table S1). To report our results in accordance to the consensus nomenclature as much as possible, we renamed some of the terms from the Heidelberg Eye Explorer software (i.e., we renamed the RNFL and RPE to NFL and RPE/BrM complex, respectively).

The Heidelberg Eye Explorer segmentation tool does delineate two bands (named PR1 and PR2) that correspond to the second and third hyperreflective outer retinal bands, which are currently referred to as the ellipsoid zone and interdigitation zone, respectively[19] (Supplementary Table S1). However, the software output does currently not provide

thickness values for the layers and zones between the ONL and the RPE/BrM complex. We, therefore, calculated thickness values for an additional layer distinct to the seven listed above: we subtracted the RPE/BrM complex from the outer retinal layers. This represents the photoreceptor inner and outer segments including the interdigitation zone. We, thus, termed it the "photoreceptor inner/outer segments+interdigitation zone," for readability abbreviated as PR-IS/OS. Please note, that PR-IS/OS is not referring to a previous name for the second hyperreflective outer retinal band, "IS/OS," as discussed in Spaide and Curcio.[24] In summary, we report eight distinct retinal layers plus three combinations of layers (IRL, ORL, overall).

It has to be noted that the IRL and ORL, as provided by the Heidelberg Eye Explorer software, mix the physiologically defined anatomic layers supplied by the retinal circulation (NFL, GCL, IPL, and INL) with those supplied by the choroidal circulation (OPL, ONL, photoreceptor inner and outer segments, and RPE/BrM).[25] One could argue that a unifying feature in the IRL (as given by the Heidelberg Eye Explorer software) is the presence of Müller cells, which are absent from the ORL. For other users of the Heidelberg Eye Explorer software, we provide our reference values for the older general population for all distinct layers as well as combinations of layers as given by this software, for the sake of completeness. For our association analyses, we focus on the eight distinct retinal layers.

Acquisition of Color Fundus Images and AMD-Grading

Color fundus photography of the central retina was conducted as described previously[20,21] by using the automatized Digital Retinography System (DRS camera) (CenterVue, Padova, Italy). Briefly, at least two color fundus images of each eye were acquired, capturing the central or the central nasal field of the retina within a 45° view, including the full macular region and optic disc. Color fundus images were exported as .jpg-files with a resolution of 2592×1944 pixels from the DRS camera and were imported into the K-DRS software, a self-developed application for image analysis.[21] If more than one image per eye was available and gradable, the image with the best quality was used (criteria on applicability for grading and quality described in Brandl et al.[21]).

To assess AMD features for each eye, the presence, size and area of drusen, pigment abnormalities (hyperpigmentation or depigmentation), GA, or neovascularization (NV) was determined using gradable color fundus images (details see Brandl et al.[21]). To classify AMD per eye, we applied the Three Continent AMD Consortium Severity Scale.[26] This system separates no AMD from mild early, moderate early, or severe early AMD stages depending on drusen size, drusen area, or the presence of pigmentary abnormalities, as well as late AMD defined as GA (area of atrophy $\geq$ circle with 350 μm in diameter, central or paracentral localization) and/or NV.[21,26]

As of today, there is no classification system beyond the traditional AMD classification fully relying on color fundus imaging for use in epidemiologic studies. There are new AMD classification systems emerging in clinical settings that rely on multimodal imaging.[5,27,28] Although promising, they lack validation in longitudinal studies as well as a universal consensus.[5] Therefore, we chose the abovementioned color fundus imaging-based system, which was recently developed by harmonizing the grading of the population-based Rotterdam Study, the Beaver Dam Eye Study, the Los Angeles Latino Eye Study, and the Blue Mountain Eye Study.[26]

Statistical Analyses for the Association of AMD Status With Retinal Layer Thicknesses

Statistical analyses were carried out using the statistical software package IBM SPSS Statistics, Version 23 (IBM, Armonk, New York, USA) and R, Version 3.4.2.[29]

We tested for differences in retinal layer thicknesses between eyes with early AMD disease stages and eyes without any AMD by using a linear mixed model for each layer separately.[30] The dependent variable of each model was the natural logarithm of manually corrected retinal layer thickness by circle (central, inner, and outer) and by eyes. The independent variables were age (linear), sex, circle, and a four-category variable for the eye's AMD stage (no, mild early, moderate early, or severe early AMD, according to the Three Continent AMD Consortium Severity Scale). One model was fitted per layer (eight distinct layers and three combinations of layers) as described above. We included an interaction effect of the four-category AMD status with macular circle (central, inner, and outer) to account for differing retinal layer thickness by circle[11] and to estimate potentially differing effects of the disease stages on retinal layer thickness in the different circles. The estimated effects of this interaction term are of main interest when analyzing differences in the retinal layer thicknesses related to AMD disease status. We included a linear effect of age and a binary effect for sex to account for potential confounding: it had been shown that, for example, overall retinal thickness,[31,32] NFL,[33,34] or other retinal layers[23] decreased with age and that eyes in men had thicker central retinas than eyes in women[23,31,32] in several studies. For each layer, the dataset consists of multiple measurements per study participant and eyes; we, thus, accounted for this correlation structure by including a participant-specific random intercept and a nested random intercept for each eye per participant into each model.

We tested for (pairwise) differences in values of the retinal layer thicknesses between AMD stages (mild early, moderate early, or severe early AMD compared to no AMD) separately for each macular circle by using approximate F-tests based on the Kenward-Rogers Approach.[35] In total, this resulted in 72 pairwise tests (3 AMD stages $\times$ 3 macular circles $\times$ 8 distinct retinal layers). We controlled the family-wise error rate by Bonferroni correction by applying a significance level of $0.05/72 = 6.94 \times 10^{-04}$. We present parametric bootstrap confidence intervals for the retinal layer thicknesses by disease stage.

In our population-based sample of older individuals, other central retinal pathologies are present that potentially influence the thickness of retinal layers independent of AMD stage (e.g., vitreoretinal boarder disorders or diabetic macular edema). These might not occur uniformly across the AMD disease stage groups in the present dataset. Therefore, we conducted a sensitivity analysis excluding eyes with early or late AMD or any other visible central retinal pathologies (such as epiretinal membranes, pathologic myopia, vascular abnormalities/bleeding, diabetic retinopathy, status postphotocoagulation, glaucomatous optic disc excavation, and also small drusen, midperipheral drusen, or any non-AMD-related pigmentary abnormalities).

Replication Study Sample and Statistical Modeling for Replication Analysis

To replicate the findings from the initial analysis, we used data from our second AugUR baseline survey. This survey is ongoing, having started in 2017, and has enabled us to generate a cross-sectional dataset of all available 546 participants (1026 eyes) without further selection other than no or

TABLE 1. Participant Characteristics*

Characteristic	All, $n = 495$		Men, $n = 243$		Women, $n = 252$	
	Values by Sex and Eye					
Age, y, mean ± SD	77.7 ± 5.2		77.6 ± 5.2		77.7 ± 5.3	
Age, y, median (IQR)	76.5 (73.4–81.1)		76.4 (73.4–81.2)		76.6 (73.4–81.1)	
AMD status†	OD	OS	OD	OS	OD	OS
No AMD, % (n)	77.6 (335)	77.0 (342)	75.2 (158)	76.1 (162)	79.7 (177)	77.9 (180)
Mild early AMD, % (n)	6.0 (26)	7.0 (31)	7.6 (16)	7.0 (15)	4.5 (10)	6.9 (16)
Moderate early AMD, % (n)	4.6 (20)	4.5 (20)	3.8 (8)	3.8 (8)	5.4 (12)	5.2 (12)
Severe early AMD, % (n)	6.5 (28)	4.5 (20)	7.6 (16)	5.6 (12)	5.4 (12)	3.5 (8)
Late AMD, % (n)	5.3 (23)	7.0 (31)	5.7 (12)	7.5 (16)	5.0 (11)	6.5 (15)
Late AMD with GA only, % (n)	1.6 (7)	2.3 (10)	1.4 (3)	1.9 (4)	1.8 (4)	2.6 (6)
Late AMD with NV only, % (n)	2.3 (10)	3.8 (17)	2.4 (5)	4.2 (9)	2.3 (5)	3.5 (8)
Late AMD with GA+NV, % (n)	1.4 (6)	0.9 (4)	1.9 (4)	1.4 (3)	0.9 (2)	0.4 (1)

* Shown are age and AMD status for the 495 analyzed participants from the first baseline survey of our AugUR OCT substudy, separately for men and women. Age ranged from 70 to 94 years in men and in women.

† AMD status was available for 464 participants (876 eyes). AMD grading was performed on color fundus images following the Three Continent AMD Consortium Severity Scale, additionally separating late AMD into GA only, NV only, and GA occurring together with NV in the same eye.[21,26]

early AMD on color fundus photography and SD-OCT-derived retinal layer thicknesses. The recruiting procedure, study protocol, and standard operating procedures for the second survey were the same as those for the first survey. Specifically, we have applied the same AMD classification. For the analysis of retinal layer thicknesses, no manual inspection or correction of retinal layer autosegmentation was conducted in the second survey data. All SD-OCT scans with values for all layers and macular subfields were included in the replication analysis. We have compared association results of the autosegmented retinal layer data from the second survey with the autosegmented retinal layer data from the first survey.

We selected the layers and circles that showed a statistically significant association with early AMD in the first survey data and tested these layers and circles in the independent second survey data by using the same linear mixed models as for the initial analysis. When the initial data analysis showed association for any early AMD stage (mild, moderate, or severe) versus no AMD, we conducted the replication analysis for each AMD stage versus no AMD to substantiate a potential trend by increasingly severe AMD stage, if possible. We considered an association with one layer/circle as replicated, when it was statistically significant in the replication data at a Bonferroni corrected level, that is three times the number of significant layers/circles tested ($n = 7$); three times since each early AMD stage was tested against no AMD. We required a significant replication to interpret and discuss the respective finding further.

RESULTS

Participant Characteristics

Of the 510 participants from the first baseline survey of our AugUR OCT substudy, 508 individuals had 49 Raster macular cube SD-OCT scans successfully acquired for at least one eye. After excluding 24 eyes from 22 participants due to mislocalization of the cube (7 eyes), low quality (10 eyes), or severe retinal pathologies (7 eyes; Methods, Supplementary Figure S1), our analyzed sample consisted of 980 eyes (489 right and 491 left eyes) from 495 participants with successfully segmented and, if necessary, manually corrected scans, that is 97.4% of eyes with acquired scans were analyzed. Of these 495 participants, 50.9% were women, age at examination ranged

from 70 to 94 years (mean, 77.7 ± 5.2 years; median, 76.5 years [interquartile range {IQR}, 73.4–81.1 years]; Table 1), and color fundus images were gradable for AMD for 464 individuals (876 eyes). These 876 eyes constituted the analyzed sample for the association between layers and AMD stages (see AMD stage frequencies in Table 1).

Retinal Layer Thicknesses in the General Older Population

Thickness values of eight distinct retinal layers plus three combinations (inner, outer, and overall retinal layers, as provided by the Heidelberg Eye Explorer software) were derived from all 980 eyes of the 495 analyzed participants separately for the central, inner, and outer circle (Fig. 1). In descriptive comparisons, retinal layer thicknesses did not differ markedly between right and left eyes (Supplementary Table S2A). For example, overall retinal layer thickness in the central circle showed a median of 279.0 μm (IQR, 262.0–295.0) for the right and 278.0 μm (IQR, 262.0–295.0) for the left eyes. We found a difference in descriptive comparisons between men and women, with a thinning in women distributed across the central and/or inner circles of all eight distinct retinal layers and the three combined layers but a thickening in the outer circles of eight of these eleven layers (Supplementary Table S2B). We detected no marked differences in descriptively comparing the 70- to 76-year-old versus the 77- to 94-year-old participants (analyzed sample divided at the median age of 76.5 years; Supplementary Table S2C).

In addition to reference values from the general older population, we also obtained reference values for "healthy" individuals aged 70+ without AMD or any other pathologic alterations detected on color fundus images (Methods); we yielded 110 eyes (58 right, 52 left) and reported thicknesses of the eight distinct retinal layers and the three combined layers, separately for central, inner and outer circles (Supplementary Table S3).

Retinal Layer Thicknesses in Early AMD

The 876 eyes (464 individuals) with retinal layer thicknesses and AMD stage available included 54 eyes with late AMD. As expected, these demonstrated notable alterations of all central retinal structures in SD-OCT segmentation; Supplementary
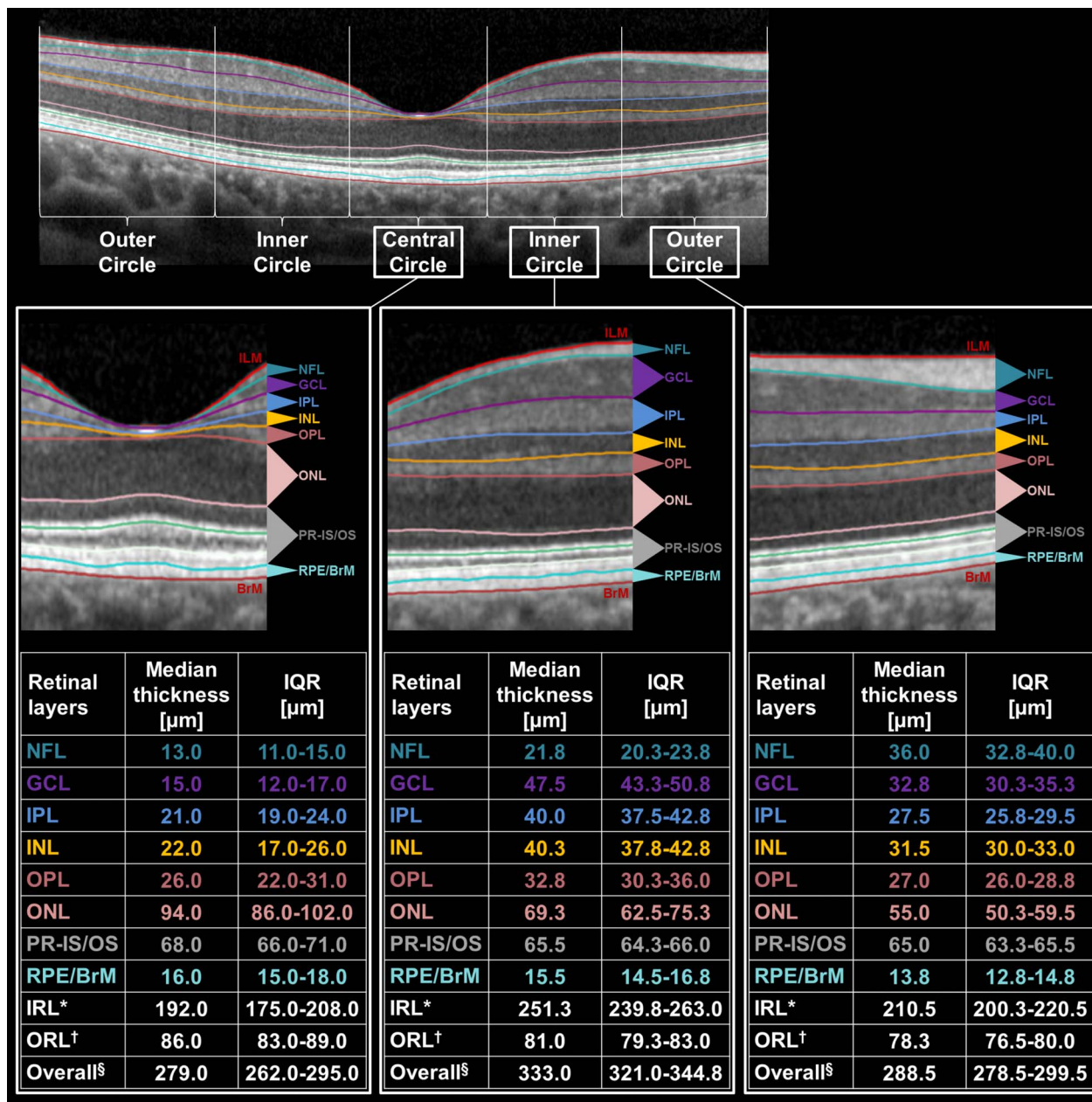
FIGURE 1. Retinal layer thicknesses in a population aged 70+. Depicted are segmented retinal layers in a horizontal foveal SD-OCT B-scan; magnifications are separated for central, inner, and outer circles (as defined by the ETDRS grid, nasal/temporal/superior/inferior subfields combined). Tables below provide median thickness values (μm) and IQRs (25th to 75th quartile) of the eight distinct retinal layers in all 495 analyzed participants (980 eyes; 489 right and 491 left) from the first baseline survey of our AugUR OCT substudy. All values given are those after manual correction of autosegmentation. *Ranging from inner limiting membrane to external limiting membrane; derived by software. †Ranging from external limiting membrane to BrM; derived by software. §Ranging from inner limiting membrane to BrM; derived by software.

Figure S2 exemplarily shows boxplots of overall retinal thickness in no, early, and late AMD stages in the central circle, revealing a thinning in GA and thickening in NV.

We excluded eyes with late AMD, yielding 822 eyes from 449 participants for further analyses, to focus on differences in retinal layer thicknesses for early AMD disease stages (57, 40, and 48 eyes for mild, moderate, and severe early AMD, respectively) compared to 677 eyes with no AMD. Results of estimated linear mixed models are illustrated in Figure 2. After Bonferroni correction for 72 pairwise tests ($P < 0.05/72 = 6.94 \times 10^{-04}$), 9 pairwise comparisons showed significant differences (Table 2): (1) RPE/BrM complex thickness was significantly increased in the central and inner circle for moderate early and severe early AMD compared to no AMD (P values between 7.23×10^{-06} and 6.41×10^{-92}); (2) PR-IS/OS and ONL thicknesses were decreased in the central circle for moderate early (PR-IS/OS, $P = 2.48 \times 10^{-05}$) or severe early (ONL, $P = 1.44 \times 10^{-06}$) AMD compared to no AMD; and (3) NFL, GCL, and IPL thicknesses were increased for mild early AMD in the central circle. The latter was inconclusive because this pattern of increased retinal layer thicknesses was not consistently observable in moderate and severe early AMD.

When restricting the control group of eyes with no AMD to eyes without any pathology on color fundus images (110 eyes, Supplementary Figure S3), all associations remained statistically significant, except the association of ONL thickness with
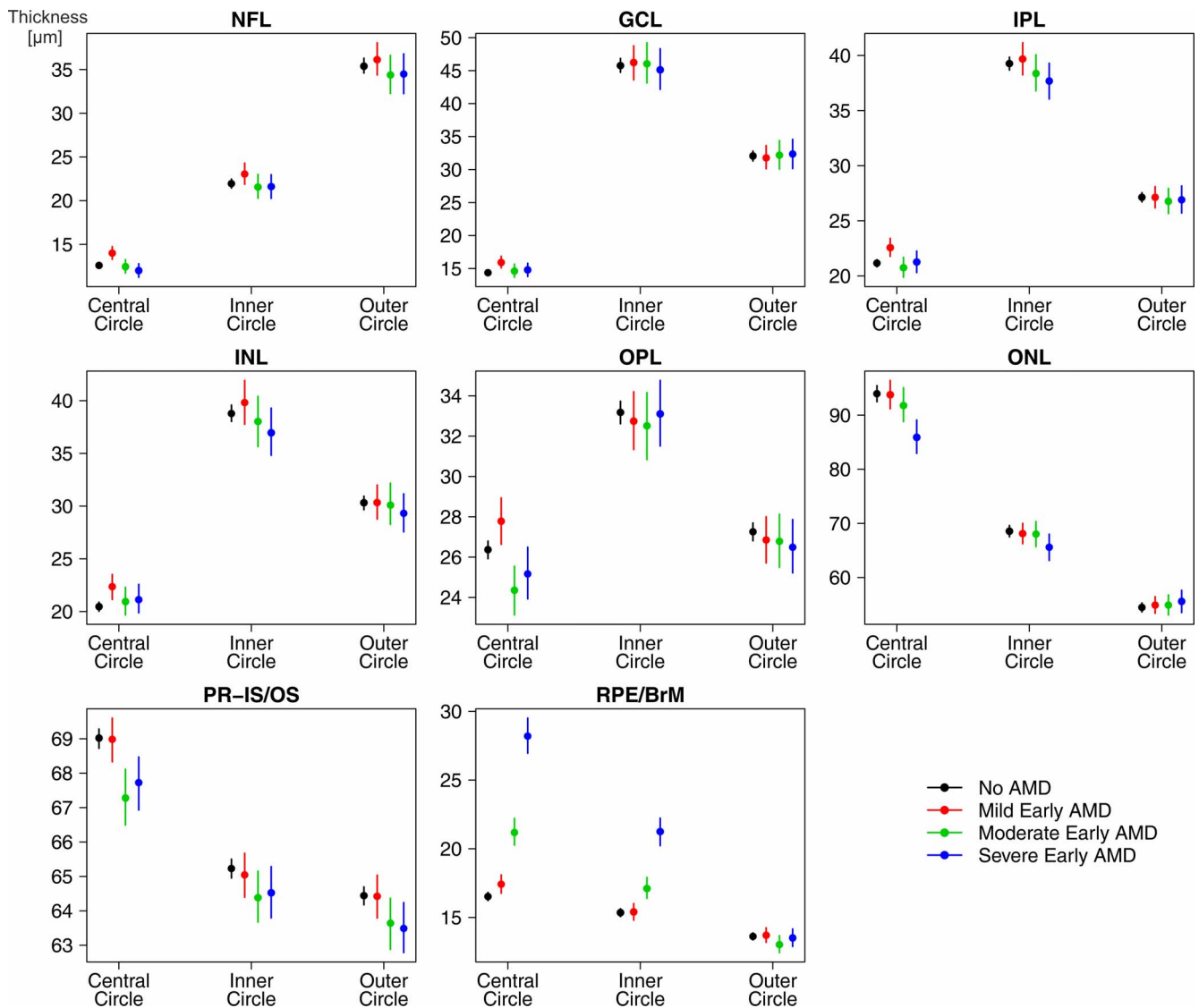
FIGURE 2. Model-based expected retinal layer thicknesses by early AMD stage. Depicted are estimates of expected retinal layer thicknesses (μm) based on layer-specific linear mixed models of 822 eyes with no AMD ($n = 677$), mild early ($n = 57$), moderate early ($n = 40$), or severe early AMD ($n = 48$) from the first AugUR baseline survey after manual correction of retinal layer segmentation. Estimates by AMD status and central, inner, and outer circles are derived from linear mixed models, adjusted for linear age and sex and nested random effects for within-person and within-eye correlation. The 95% confidence intervals are derived from model-based parametric bootstrap.

TABLE 2. Retinal Layer Thicknesses With Significant Difference Between No and Early AMD Stages*

	Expected Retinal Layer Thicknesses, μm				Effect Estimates ($\hat{\beta}$)/Pairwise Test *P* Value		
Retinal Layers	No AMD ($n = 677$)	Mild Early AMD ($n = 57$)	Moderate Early AMD ($n = 40$)	Severe Early AMD ($n = 48$)	Mild Early vs. No AMD	Moderate Early vs. No AMD	Severe Early vs. No AMD
NFL, central circle	12.6	14.0	12.4	12.0	**0.10 / 5.67 × 10^{-05}**	−0.01 / 0.69	−0.05 / 0.13
GCL, central circle	14.4	15.9	14.6	14.8	**0.10 / 1.82 × 10^{-04}**	0.02 / 0.62	0.03 / 0.37
IPL, central circle	21.2	22.6	20.7	21.3	**0.06 / 3.31 × 10^{-04}**	−0.02 / 0.38	0.01 / 0.82
ONL, central circle	93.9	93.8	91.8	85.9	0.00 / 0.91	−0.02 / 0.17	**−0.09 / 1.44 × 10^{-06}**
PR-IS/OS†, central circle	69.0	69.0	67.3	67.7	0.00 / 0.91	**−0.03 / 2.48 × 10^{-05}**	−0.02 / 1.51 × 10^{-03}
RPE/BrM, central circle	16.5	17.4	21.2	28.2	0.05 / 0.01	**0.25 / 1.81 × 10^{-24}**	**0.54 / 6.41 × 10^{-92}**
RPE/BrM, inner circle	15.3	15.4	17.1	21.2	0.00 / 0.87	**0.11 / 7.23 × 10^{-06}**	**0.32 / 8.58 × 10^{-38}**

* Shown are estimates of expected retinal layer thicknesses [μm], effect estimates ($\hat{\beta}$, on log scale), and P-values of pairwise tests (mild, moderate, severe early AMD vs no AMD) from layer-specific linear mixed models. These results are based on 822 eyes from the first AugUR baseline survey after manual correction, excluding eyes with late AMD. P values were judged at Bonferroni-corrected significance level, $P < 0.05/72 = 6.94*10^{-04}$. Significant results are highlighted with bold text.

† Ranging from external limiting membrane to RPE; self-calculated.

TABLE 3. Retinal Layers Requiring Manual Correction*

Retinal Layers	Number of Eyes Requiring Manual Correction, % (Total = 980 Eyes)	Fraction of Changed Mean Thickness Measurements From Manual Correction, % (Total = 2466 Thickness Measurements per Layer)
NFL	693 (70.71)	31
GCL	697 (71.12)	35
IPL	673 (68.67)	44
INL	622 (63.47)	43
OPL	330 (33.67)	37
ONL	287 (29.29)	21
PR-IS/OS†	201 (21.43)	29
RPE/BrM	276 (28.16)	23

* Listed are (1) all layers that had to be manually corrected for segmentation errors in any portion of at least one of the 49 cross-sectional images. It has been taken into account that a layer is defined by two lines delineating the upper and lower optical reflectivity boundaries. Therefore, a layer has been marked as manually corrected, if either the upper and/or lower line has been edited. Results are given for the 980 eyes of the 495 analyzed participants from the first AugUR baseline survey. (2) The fraction of mean retinal layer thickness measurements that are changed by the manually corrected retinal layer segmentation. Considered here are the 2466 observed measurements per layer that make up the database for the linear mixed models (3 circles in 822 considered eyes with no or early AMD from the first AugUR baseline survey).

† Ranging from external limiting membrane to retinal pigment epithelium; self-calculated.

severe early AMD in the central circle, and a new association for increased ONL thickness with severe early AMD in the outer circle emerged ($P = 2.88 \times 10^{-04}$).

On the Necessity of Manually Correcting the Automated Retinal Layer Segmentation

Of the 980 eyes analyzed, 760 eyes (77.6%) required manual correction of autosegmentation errors in at least one line in any portion of at least one of the 49 cross-sectional images. Some layers were more prone to segmentation errors than others (Table 3): more frequent manual correction was required for inner layers, such as the GCL (71.1% of the 980 eyes) and the NFL (70.7% of the 980 eyes), compared to outer layers, such as the ONL (29.3%) or the RPE/BrM complex (28.2%).

This high percentage of segmentation errors raises concern about whether results of the autosegmentation are usable without manual inspection and correction. In our present analysis, we relied on the measurements derived from manually corrected segmentation; however, the question arises whether this was necessary to detect the association of layers with AMD stages and whether the difference between corrected and autosegmented values was relevant on the population level. We, thus, quantified the differences in layer thicknesses derived from the automated (error-prone) and manually adjusted (assumed as correct) retinal layer segmentation to shed light on the extent of the measurement error and its consequences on association results (Supplementary Text S1).

We found several differences in retinal layer thicknesses between automated and manually corrected segmentation (Fig. 3). Particularly for the RPE/BrM complex, the segmentation error became more pronounced with increasing disease severity. This was in line with our visual impression that the automated segmentation often failed to localize BrM correctly in the presence of, for example, drusen (Fig. 4). When analyzing the association of autosegmented layer thicknesses with early AMD stages, we found the same significant associations as reported above by using the manually corrected layers thicknesses (Table 4; Fig. 5). Additionally, a significant thinning of PR-IS/OS in severe early AMD versus no AMD ($P = 2.91 \times 10^{-06}$; Table 4) was observed for autosegmented data that was not significant in the manually corrected data ($P = 1.51 \times 10^{-03}$; Table 2). However, we did observe biased association estimates, particularly for the comparison of the RPE/BrM complex in no AMD with moderate/severe early AMD (bias toward the null, Fig. 5).

Independent Replication of Differences in Retinal Layer Thicknesses Between No AMD and Early AMD Stages

To replicate our findings in an independent dataset, we used the data from the second AugUR baseline survey (Methods). This analysis consisted of 546 individuals (1026 eyes; 514 right, 512 left) with retinal layer thickness values from autosegmented SD-OCT scans for at least one eye as well as no AMD or early AMD based on color fundus images applying the Three Continent AMD Consortium Severity Scale. In this second independent AugUR data, age at examination ranged from 70 to 95 years (mean, 78.3 ± 5.0 years; median, 77.7 years [IQR, 74.3–81.6 years]) and 58.2% ($n = 310$) were women, similar to the first survey data. In this replication dataset, a total of 836 eyes revealed no AMD and 72 eyes showed mild early, 72 moderate early, and 46 severe early AMD. We analyzed the association of each of the three early AMD stages versus no AMD with thicknesses in these retinal layers and circles, for which we had detected a significant finding in the first dataset. This resulted in testing seven layers/circles for each of the three AMD stages, and we, thus, judged significance in the replication data at the Bonferroni-corrected level of $0.05/21 = 2.38 \times 10^{-03}$ (Methods).

We compared association results from the replication data for autosegmented layer thicknesses with autosegmented thicknesses from the first dataset and found the following (Table 4): (1) as before, RPE/BrM complex thickness was significantly increased in the central and inner circle for moderate early and severe early AMD compared to no AMD (P values between 1.72×10^{-08} and 9.38×10^{-36}). We even detected a significant association for mild early AMD versus no AMD with this layer in the central circle ($P = 9.11 \times 10^{-05}$), which was not observed in our initial data (neither with the autosegmented nor with the manually corrected thickness values). (2) As before, PR-IS/OS and ONL thicknesses were decreased in the central circle for moderate early (PR-IS/OS, $P = 3.68 \times 10^{-05}$) or severe early AMD (ONL, $P = 8.24 \times 10^{-04}$), respectively, and now, in the second dataset, even for mild early AMD versus no AMD for ONL ($P = 1.50 \times 10^{-04}$). Moreover, the replication data revealed a tendency toward a thinner PR-IS/OS in severe early AMD versus no AMD ($P = 0.028$), which was similar to our observation in the initial data ($P = 2.91 \times 10^{-06}$ for autosegmented and $P = 1.51 \times 10^{-03}$ for manually corrected thickness values). (3) NFL, GCL, and IPL thicknesses did not reveal any statistically significant difference
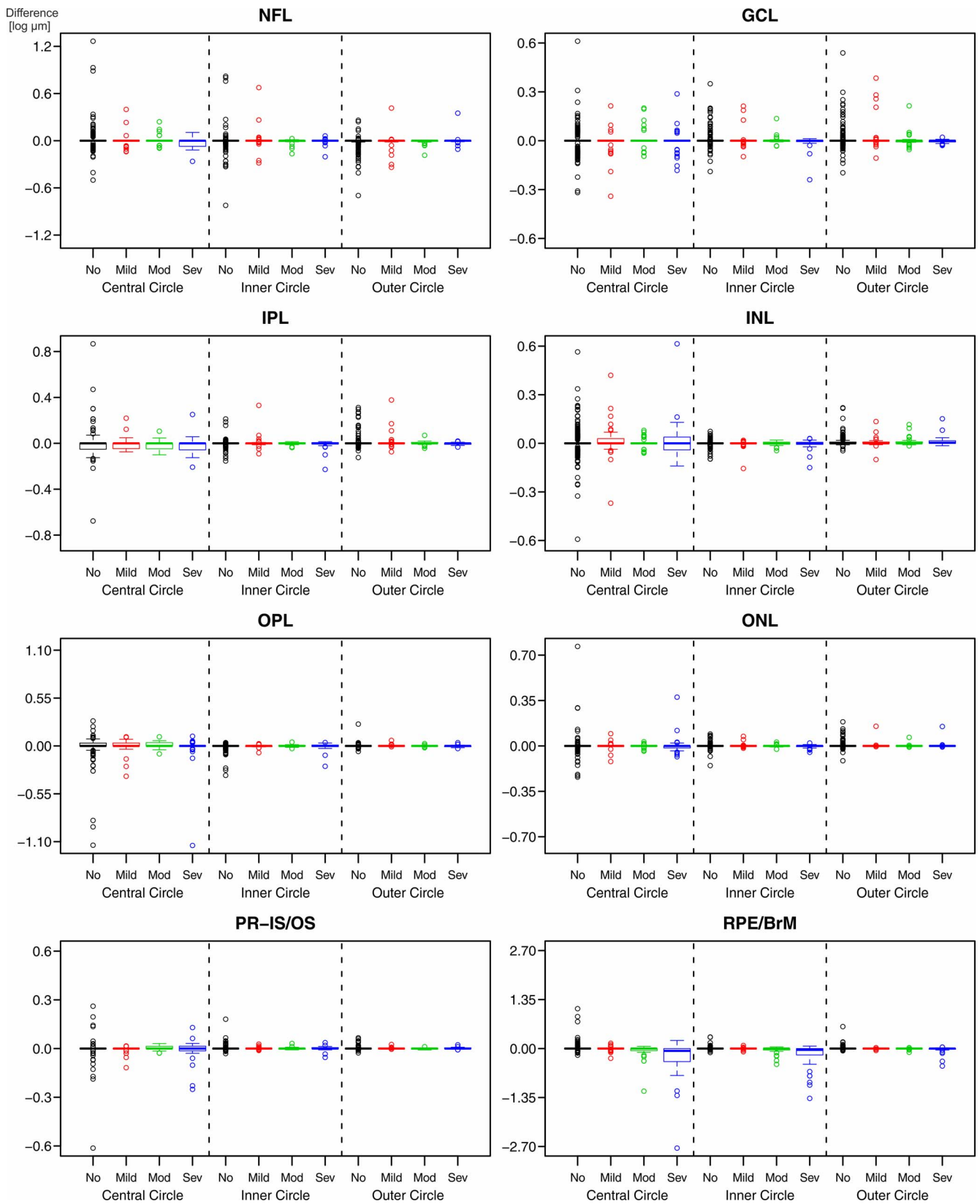
FIGURE 3. Differences in retinal layer thicknesses derived from automated and manually corrected segmentation. Boxplots show differences between the logarithmic retinal layer thicknesses obtained from automated segmentation and manual correction. Negative/positive values indicate measurement error toward too small/big thicknesses. Note the differing *y*-axis scale between layers.
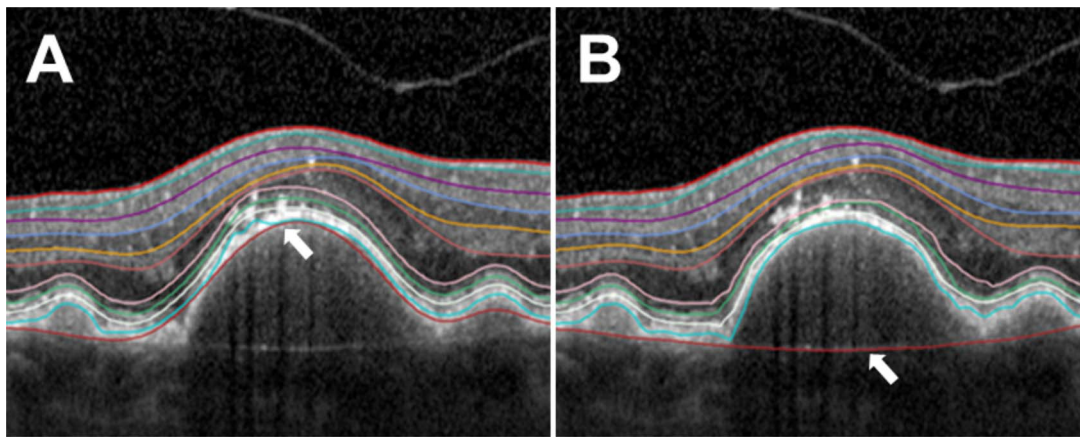
FIGURE 4. Example of autosegmentation error. Depicted are (**A**) the mislocalized BrM (*lower red line*, *white arrow*) in automated segmentation and (**B**) the corresponding manual correction (*white arrow*) in a horizontal macular SD-OCT scan revealing severe early AMD with large drusenoid pigment epithelial detachment.

for any early AMD stage versus no AMD in the replication analysis; for these layers, the initial data had shown a significant thickening when comparing mild early versus no AMD, which was not consistently observable in moderate and severe early AMD.

We, thus, conclude that we robustly identified a thickening of the RPE/BrM complex in the central and inner circle and a thinning of ONL and PR-IS/OS in the central circle for individuals with early AMD stages compared to no AMD.

DISCUSSION

Here, we present a systematic evaluation of retinal layer thicknesses assessed via Spectralis SD-OCT segmentation software, including manual correction in a population-based study of 495 older individuals (age range, 70 to 94 years). There are three important aspects of our work. First, we provide data on the reliability of retinal layer segmentation using the Spectralis SD-OCT software by comparing autosegmented retinal layer thicknesses with manually corrected values. Second, by linking each of the retinal layer thicknesses with color fundus imaging-based early AMD stages in the so far first dataset of this kind, we were able to pinpoint the specific layers that were associated with mild, moderate, or severe stages of early AMD. Our findings that the RPE/BrM complex was thicker and the PR-IS/OS and ONL were thinner for eyes with moderate or severe early AMD compared to eyes with no AMD highlight these retinal layers as potential quantitative imaging biomarkers of early AMD. Importantly, we were able to replicate these findings in an even larger, independent, yet comparable replication sample including >500 persons. Third, given our population-based study design, we can also provide reference values for retinal layer thicknesses for an older population or Caucasian ancestry, which fills a current gap of data.

Reference Values for Retinal Layer Thicknesses in a Population Aged 70+

With regard to reference values, there are several previous works on overall retinal thickness[31,32,36] and some work on the thicknesses of single retinal layers, such as the RPE[13] or NFL,[34] from large population-based studies. Won et al.[23] provided Spectralis SD-OCT-based retinal layer thickness values for Asians (50 healthy Koreans, hospital-based recruitment, 20 to 80 years of age). However, overall retinal thickness has been shown to differ between ethnicities,[36,37] and layer-specific reference values for European ancestry were still lacking. Szigeti et al.[38] provided layer-specific thickness values for Caucasians (53 healthy individuals, hospital-based recruitment, 6 to 67 years of age) applying the Stratus OCT device (Zeiss), but overall retinal thickness has been shown to differ between devices.[39–41] These differences must be considered when referring to our proposed reference values from Spectralis SD-OCT. Here, we present the full distribution of thickness values for all retinal layers as given by Spectralis SD-OCT in a mobile population aged 70+ and the distribution among those without AMD or any other pathologic alterations on color fundus images. Our study provides the first population-based data on all retinal layer thicknesses, as given by Spectralis SD-OCT and the first in European-ancestry individuals.

Association of Early AMD With Thicknesses of RPE/BrM Complex and Photoreceptor Layers

This present study is the first to assess the association of early AMD with all retinal layer thicknesses as provided by the Spectralis SD-OCT in two population-based surveys totaling nearly 1000 individuals and >1800 eyes. Notable previous efforts with smaller sample sizes focused on either inner[7] or outer[6,17,18] retinal layers. Our investigation revealed two important results. First, our finding of a thickening of the RPE/BrM complex by early AMD stages fits well to the notion that this layer is enlarged by accumulating extracellular debris in the subretinal space (subretinal drusenoid deposits), internal to the RPE basal lamina (basal laminar deposits), and/or external to the RPE basal lamina (basal laminar deposits/drusen).[2,3,42] This confirms previous data by the Age-Related Eye Disease Study 2 Ancillary SD-OCT Study (269 persons with advanced early AMD vs. 115 controls),[6] where the RPE was investigated specifically without analyzing this in the context of the other retinal layers.

Second, our finding of a thinning of the photoreceptor layers PR-IS/OS and ONL is important due to the fact that this is already seen in early AMD stages and not only after onset of late AMD. We found these decreased ONL and PR-IS/OS thicknesses assessed as mean within circles in 88 moderate/severe early AMD eyes compared to 677 eyes with no AMD and replicated the finding in further 118 moderate/severe early AMD eyes compared to 836 eyes with no AMD, providing evidence from a total of 206 versus 1513 eyes. Our finding complements previous results from two studies showing a

TABLE 4. Replication of Effect Estimates of No and Early AMD Stages on Retinal Layer Thicknesses*

Retinal Layers	Initial Analysis Automatically Segmented ($n = 822$)			Replication Automatically Segmented ($n = 1026$)		
	Mild Early vs. No AMD	Moderate Early vs. No AMD	Severe Early vs. No AMD	Mild Early vs. No AMD	Moderate Early vs. No AMD	Severe Early vs. No AMD
NFL, central circle	**0.10 / 2.48 $\times 10^{-04}$**	-0.01 / 0.82	-0.08 / 0.03	-0.04 / 0.20	-0.02 / 0.54	0.02 / 0.68
GCL, central circle	**0.10 / 4.43 $\times 10^{-04}$**	0.03 / 0.43	0.04 / 0.29	-0.04 / 0.19	0.00 / 0.94	0.04 / 0.34
IPL, central circle	**0.07 / 4.29 $\times 10^{-04}$**	-0.02 / 0.39	-0.01 / 0.82	-0.02 / 0.32	0.00 / 0.98	0.03 / 0.25
ONL, central circle	0.00 / 0.83	-0.02 / 0.20	**-0.09 / 2.03 $\times 10^{-06}$**	**-0.06 / 1.50 $\times 10^{-04}$**	-0.05 / 5.00*10^{-03}	**-0.07 / 8.24 $\times 10^{-04}$**
PR-IS/OS‡, central circle	0.00 / 0.30	**-0.02 / 7.65 $\times 10^{-05}$**	**-0.03 / 2.91 $\times 10^{-06}$**	-0.01 / 0.17	**-0.02 / 3.68 $\times 10^{-05}$**	-0.01 / 0.028
RPE/BrM, central circle	0.04 / 0.02	**0.18 / 1.64 $\times 10^{-17}$**	**0.32 / 5.90 $\times 10^{-49}$**	**0.06 / 9.11 $\times 10^{-05}$**	**0.21 / 6.27 $\times 10^{-31}$**	**0.29 / 9.38 $\times 10^{-36}$**
RPE/BrM, inner circle	0.00 / 0.98	**0.07 / 4.71 $\times 10^{-04}$**	**0.19 / 2.09 $\times 10^{-19}$**	0.00 / 0.80	**0.10 / 1.72 $\times 10^{-08}$**	**0.19 / 7.07 $\times 10^{-17}$**

* Shown are effect estimates ($\hat{\beta}$, on log scale) and pairwise test P values from linear mixed models. These results are based on (1) 822 automatically segmented eyes of the initial analysis ($n = 677$ no AMD, $n = 57$ mild early, $n = 40$ moderate early, and $n = 48$ severe early AMD) and (2) 1026 automatically segmented eyes of the replication sample ($n = 836$ no AMD, $n = 72$ mild early, $n = 72$ moderate early, and $n = 46$ severe early AMD). P values were judged at Bonferroni-corrected significance level, $P < 0.05/72 = 6.94 \times 10^{-04}$ for initial analysis and $P < 0.05/21 = 2.38 \times 10^{-03}$ for replication analysis. Significant results are highlighted with bold text.

† Ranging from external limiting membrane to retinal pigment epithelium; self-calculated.

focal thinning of photoreceptor layers over drusen in 17 or 63 non-NV AMD eyes, respectively.[43,44] This thinning can stem from accumulating extracellular debris enlarging the neighboring RPE/BrM complex and a consecutive squishing of ONL and/or PR-IS/OS or from photoreceptor cell loss/damage already at early-disease stage. The latter would be highly interesting, as this would implicate changes of photoreceptor layers early in the disease process, whereas a photoreceptor loss is currently seen as the key feature of late AMD.[2] The hypothesis of a photoreceptor cell loss/damage early in the AMD disease process is supported by structural data from postmortem investigations of photoreceptor cell loss in five midstage non-NV AMD eyes[45] and by functional data on delayed rod-mediated dark adaptation[46] also indicating photoreceptor damage very early in the AMD disease process. A visual function study in 21 early AMD eyes also showed a thinning of the photoreceptor outer segment layer in SD-OCT to be associated with decreased visual sensitivity (i.e., visual field defects).[47]

It is interesting to note that we observed these associations for the RPE/BrM complex, ONL, and PR-IS/OS only in the central and/or inner circle; this is in line with the foveal region being the primary place of AMD pathology.[2] Besides, the significant thinning of PR-IS/OS in moderate early versus no AMD was not found consistently in severe early versus no AMD (significant in the autosegmented data of our initial data but not in the manually corrected nor in the autosegmented values of our replication data). We do not have a compelling biological hypothesis for an effect in moderate but not in severe early versus no AMD. It might be possible that the effect we found in moderate early versus no AMD could be due to errors in the segmentation. However, we do have a strict control for multiple testing to guard against false positive findings, which increases the probability for false negatives. It is perceivable that there is a true effect also for severe early AMD versus no AMD for this layer, which was missed in the present analysis.

Overall, our systematic approach enabled a joint view on the RPE/BrM complex and the photoreceptor layers in a relatively large sample size, putting these layer thicknesses on spot as potentially useful quantitative imaging biomarkers of moderate and severe early AMD. Thus, thicknesses of the RPE/BrM complex and photoreceptor layers could extend the list of reported (qualitative) imaging biomarkers, such as hyperreflective foci,[48] the different types of drusen/deposits (especially subretinal drusenoid deposits[3,5]), and several others.[5] Furthermore, the thicknesses of these layers could be related to functional biomarkers, for example delayed rod-mediated dark adaptation.[46,18,49] Importantly, our data substantiate the idea of photoreceptor cell loss early in the AMD disease process.

On the Relevance of the Detected Effect Sizes

It is important to reflect the detected effect sizes for the association of early AMD with the RPE/BrM complex and photoreceptor layer thicknesses in terms of relevance. One approach is to compare effect sizes to the variability of thicknesses in our data. We exemplify effect sizes on our smallest and largest association findings: for the PR-IS/OS central circle thickness, we estimated a difference of −1.7 μm between moderate early and no AMD (Table 2). When comparing this effect to the observed IQR of 5.0 μm (Fig. 1), the absolute values of this effect size correspond to 34% of observed IQR. On the log scale ($\hat{\beta} = -0.03$ log μm; Table 2), the effect size corresponds to 46% of the SD (SD on log scale, 0.056 μm). For the RPE/BrM central circle thickness, the estimated difference is +11.7 μm between severe early and no AMD
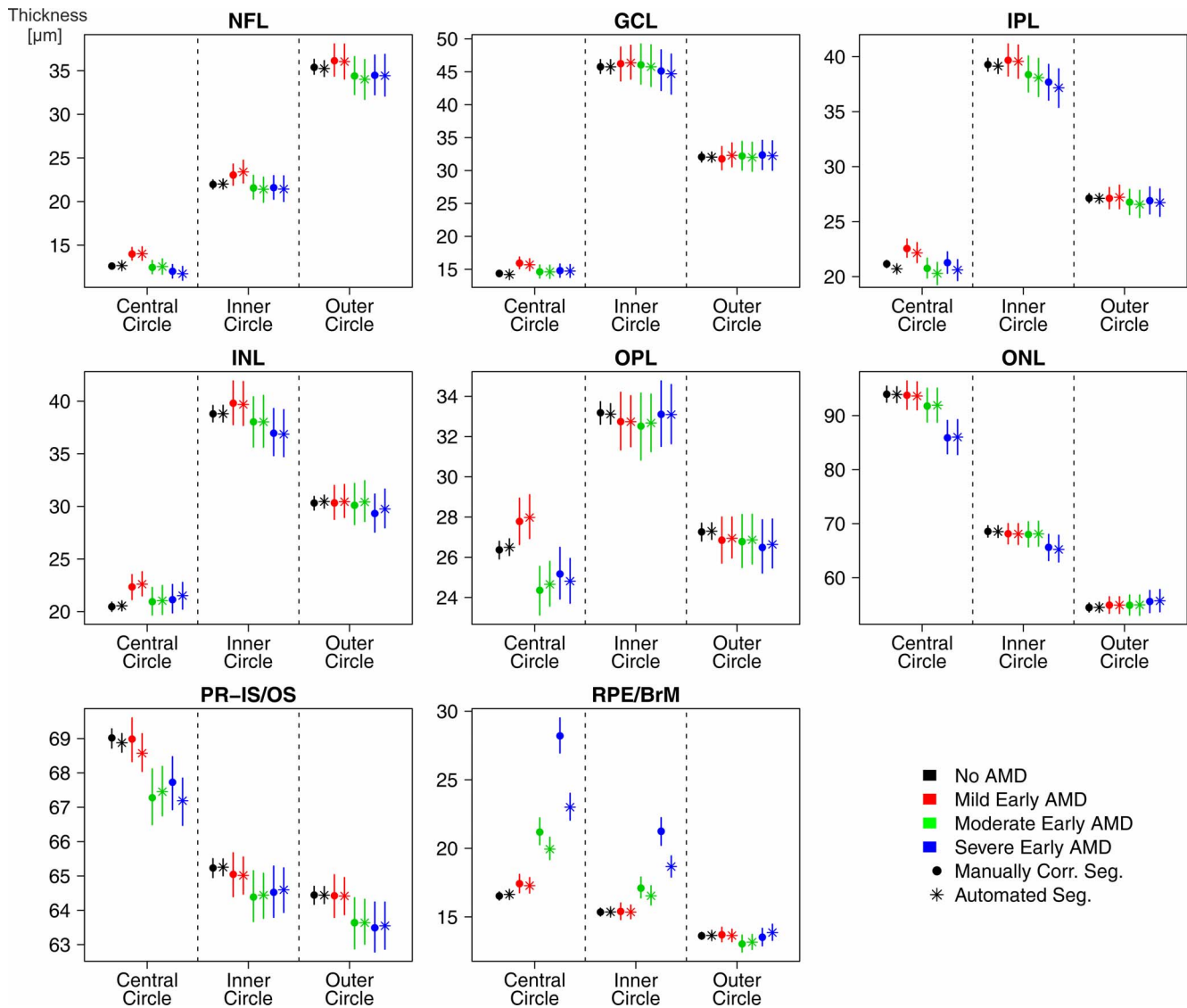
FIGURE 5. Comparison of expected retinal layer thicknesses in early AMD derived from automated and manually corrected segmentation. Depicted are estimates of expected retinal layer thicknesses (μm) from automated (*asterisk*) and manually corrected segmentation (*circle*). Estimates are based on layer-specific linear mixed models of 822 eyes from the first AugUR baseline survey with no AMD ($n = 677$), mild early ($n = 57$), moderate early ($n = 40$), or severe early AMD ($n = 48$). Estimates by AMD status and central, inner, and outer circles are derived from linear mixed models, adjusted for linear age and sex and nested random effects for within-person and within-eye correlation. The 95% confidence intervals are derived from model-based parametric bootstrap.

(Table 2). This effect size corresponds to almost four times the IQR of 3.0 μm (Fig. 1) or, on the log scale, two times the observed SD ($\hat{\beta} = 0.54$ log μm; Table 2; SD on log scale, 0.26 μm).

It is also interesting to compare effect sizes to reported effects of other factors influencing retinal layer thicknesses. Although there is no epidemiologic data on PR-IS/OS or ONL thickness, there is data from UK Biobank for RPE in persons aged 46 to 69 years[13]; among the factors with the largest effects were ethnicity (black vs. white, 3.3 μm) and refraction (0.28 μm per diopter [D] increase, i.e., a difference of 8×0.28 μm = 2.2 μm comparing persons with +4D to −4D at the ends of the refractive status interval containing ~95% of UK Biobank individuals). Thus, our observed effect of severe early AMD on RPE/BrM central circle thickness of 11.7 μm (Table 2) was ~5 times higher than the reported effect from +4D/−4D and 3.5 times higher than the reported effect from black/white ethnicity.

A Discussion of Potential Confounders

In our association analysis, we were able to consider all observed eyes, for which SD-OCT layer segmentation was available, by accounting for the multiple measurements per participant and layer (within and between eyes) in linear mixed models. We adjusted for age and sex, as these are not only associated with AMD[2] but also with overall retinal thickness,[31,32] NFL,[33,34] or other retinal layers.[23] However, we need to acknowledge the lack of assessing axial length (AL) and/or refraction in our study and the lack of accounting for these factors in our association models. On the one hand, it has been shown that the actually measured micrometer for thickness values using SD-OCT are not compromised by AL or refraction,[50] at least in single thickness measurements (e.g., using a longitudinal reflectivity profile) in a single B-scan but not necessarily in thickness measurements over a particular area, such as subfields of an ETDRS grid. On the other hand,

when AL or refraction is associated with early AMD and retinal layer thicknesses, these factors are potential confounders of an association of early AMD and retinal layer thicknesses, which we discuss in the following paragraph.

Increased AL has been shown to be associated with lower odds of (any) AMD (odds ratio OR, 0.76 per mm increase in AL).[51] Although there is substantial data on AL and overall retinal thickness,[31,52] the transferability to single layer thicknesses is unclear. There is only little data on AL and single layer thickness values; Szigeti et al.[38] showed an association of increased AL with decreased outer circle ONL thickness (r = −0.448), but no association with central circle ONL or RPE in any circle (clinic-recruited 53 healthy individuals aged 6–67 years). As a note of caution, the informativeness of this single study might be limited due to sample size and selection.

With regard to refractive status, hyperopia was shown to be associated with higher risk of (any) AMD (e.g., meta-analysis: OR = 1.09 per D; OR = 1.09^8 = 1.99 comparing +4D vs. −4D)[51] and with thicker RPE (+2.2 μm comparing +4D to −4D, see above).[13] Thus, our finding of early AMD being associated with a thicker RPE/BrM complex needs to be considered as confounded by refractive status to some extent. For a rough assessment of the extent of this confounding effect, we consider an extreme scenario: let us assume that all analyzed AugUR participants had a refractive status of either −4D or +4D and all participants with −4D had no AMD and those with +4D had early AMD. This would yield a spurious association of early AMD with RPE/BrM thickness of ∼2.2 μm, which is much smaller than our observed difference of 11.7 μm. Still, this scenario implies a (nearly indefinitely) huge OR of +4D/−4D on early AMD, whereas the reported OR is 1.99 comparing +4D/−4D, suggesting that any confounding effect is substantially smaller than 2.2 μm. There are no data on the association of refractive status with ONL or PR-IS/OS, so far, so it is difficult to judge on that end.

In summary, we acknowledge the potential of AL or refractive status to be a confounder in the associations that we detected. However, the partially available data suggest that the extent of the confounding is small compared to our observed differences.

On the Reliability of Autosegmentation Compared to Manually Corrected Segmentation

One focus of our investigation was the reliability of retinal thickness values derived from autosegmentation via Spectralis SD-OCT. A main finding of our analysis was the high percentage of observed autosegmentation errors (77.6% of eyes) as observed previously,[7] which raises concern on the utility of autosegmentation without manual correction. When quantifying the extent of the segmentation error and its consequences on the association of early AMD with retinal layer thicknesses, we found the following: (1) segmentation errors become (in some layers) more pronounced with increasing disease severity; (2) we found the same significant associations when using the autosegmented compared to the manually corrected layer thicknesses; (3) we did observe biased association estimates when using the autosegmented layer thicknesses; particularly when comparing the RPE/BrM complex in eyes with no AMD to eyes with moderate/severe early AMD, the association was underestimated with automated thickness values.

Our findings have implications for epidemiologic studies using autosegmented retinal layer thicknesses; response measurement error associated with covariates can lead to biased effect estimates with false positive or false negative associations. In principle, there are statistical approaches to correct for response measurement error in association

analyses, when internal validation data are available (i.e., autosegmented and manually corrected layer thicknesses for a subset of participants).[53,54] However, we are not aware of any ready approach for considering response measurement error associated with covariates in linear mixed models. Overall, we were able to determine the extent of measurement error from autosegmentation versus manually corrected segmentation.

We conclude that autosegmented retinal layer thickness values are reasonable but with some measurement error compared to manually corrected values, and we recommend cautious interpretation of results relying purely on autosegmented layer thicknesses. Although manually corrected thickness values are more reliable than autosegmented values, statistics for association analyses are more reliable in large studies and manual correction is not feasible in large sample sizes. One classic approach to overcome the pay-off between reliability of measurement and sample size is an internal validation subset using manual correction on top of autosegmentation to help understand differences in a specific study. Our initial data can be considered an internal validation data when viewing both AugUR surveys as one large study, which allows us to evaluate autosegmented values in the second survey with a clear feel for how this translates to manually corrected values. Our population-based data with both manually corrected and autosegmented values may also serve as external validation for comparable population-based studies, but this may not be suitable for all other studies, particularly those that focus on patients.

Limitations and Strengths of our Analyses

A technical limitation that we need to note is the inability of the Spectralis SD-OCT and the Heidelberg Eye Explorer software to automatically delineate, segment, and provide thickness values for all retinal layers/zones, as determined in the consensus nomenclature.[19] For example, it does not support the segmentation of the Henle's fiber layer (HFL), that is the axons of photoreceptor nuclei. Moreover, a particular SD-OCT imaging method is required to distinguish HFL from true ONL by altering the beam entry position (also termed directional OCT)[55,56]; we did not apply this technique; therefore, HFL is not readily visible on AugUR images and, consequently, we refrained from trying to manually delineate HFL, which would have been too error-prone. We acknowledge that the recognition of the optical properties of HFL could help gain a more thorough understanding of the retina in health and macular pathology.[55,56]

A clear strength of our study is the population-based design with an age range of 70 to 95 years. This is ideal for assessing AMD, as a reasonably large number of early AMD cases is observed, amounting to approximately 100 individuals for each of the three early AMD stages in our two datasets. Another strength is the replication of our findings from the first AugUR survey in independent but highly comparable data from our second AugUR baseline survey featuring the same protocols for recruiting, study conduct, and measurements. By this, we expanded our data from 449 individuals by another >500 and our results from two surveys and nearly 1000 participants in total can be deemed particularly solid.

Summary and Outlook

Here, we provide the first systematic data on thicknesses of all retinal layers, as provided by the Spectralis SD-OCT in a population-based study of individuals aged 70+ and their associations with early AMD stages. Importantly, our cross-sectional analysis reveals quantitatively measurable changes in the RPE/BrM complex, ONL, and PR-IS/OS in eyes with early

AMD compared to those without AMD. Our structural finding of quantifiable photoreceptor layer thinning in SD-OCT in early AMD stages supports data on decreased visual function,[46,49] which also point toward pathologic processes affecting photoreceptors very early in the AMD disease process. If this hypothesis of cell damage already at early AMD stages will be substantiated further, this might have implications for therapy. Longitudinal data are warranted to evaluate whether retinal layer thickness changes in early AMD can predict progression to late AMD independently of early AMD stages. When substantiated by longitudinal studies, thicknesses of photoreceptor layers and the RPE/BrM complex might be worth considering as potential quantitative imaging biomarkers for early AMD and its progression to late AMD.

References

1. Augood CA, Vingerling JR, de Jong PT, et al. Prevalence of age-related maculopathy in older Europeans: the European Eye Study (EUREYE). *Arch Ophthalmol*. 2006;124:529–535.

2. Lim LS, Mitchell P, Seddon JM, Holz FG, Wong TY. Age-related macular degeneration. *Lancet*. 2012;379:1728–1738.

3. Huisingh C, McGwin G Jr, Neely D, et al. The association between subretinal drusenoid deposits in older adults in normal macular health and incident age-related macular degeneration. *Invest Ophthalmol Vis Sci*. 2016;57:739–745.

4. Spaide RF, Ooto S, Curcio CA. Subretinal drusenoid deposits AKA pseudodrusen. *Surv Ophthalmol*. 2018;63:782–815.

5. Garrity ST, Sarraf D, Freund KB, Sadda SR. Multimodal imaging of nonneovascular age-related macular degeneration. *Invest Ophthalmol Vis Sci*. 2018;59:AMD48–AMD64.

6. Farsiu S, Chiu SJ, O'Connell RV, et al. Quantitative classification of eyes with and without intermediate age-related macular degeneration using optical coherence tomography. *Ophthalmology*. 2014;121:162–172.

7. Muftuoglu IK, Ramkumar HL, Bartsch DU, Meshi A, Gaber R, Freeman WR. Quantitative analysis of the inner retinal layer thicknesses in age-related macular degeneration using corrected optical coherence tomography segmentation. *Retina*. 2018;38:1478–1484.

8. Forte R, Querques G, Querques L, Massamba N, Le Tien V, Souied EH. Multimodal imaging of dry age-related macular degeneration. *Acta Ophthalmol*. 2012;90:e281–e287.

9. Abdelfattah NS, Zhang H, Boyer DS, et al. Drusen volume as a predictor of disease progression in patients with late age-related macular degeneration in the fellow eye. *Invest Ophthalmol Vis Sci*. 2016;57:1839–1846.

10. Ferrara D, Silver RE, Louzada RN, Novais EA, Collins GK, Seddon JM. Optical coherence tomography features preceding the onset of advanced age-related macular degeneration. *Invest Ophthalmol Vis Sci*. 2017;58:3519–3529.

11. Grover S, Murthy RK, Brar VS, Chalam KV. Normative data for macular thickness by high-definition spectral-domain optical coherence tomography (Spectralis). *Am J Ophthalmol*. 2009; 148:266–271.

12. Keane PA, Grossi CM, Foster PJ, et al. Optical coherence tomography in the UK Biobank study - rapid automated analysis of retinal thickness for large population-based studies. *PLoS One*. 2016;11:e0164095.

13. Ko F, Foster PJ, Strouthidis NG, et al. Associations with retinal pigment epithelium thickness measures in a large cohort: results from the UK Biobank. *Ophthalmology*. 2017;124:105–117.

14. Chan A, Duker JS, Ishikawa H, Ko TH, Schuman JS, Fujimoto JG. Quantification of photoreceptor layer thickness in normal eyes using optical coherence tomography. *Retina*. 2006;26: 655–660.

15. Chan A, Duker JS, Ko TH, Fujimoto JG, Schuman JS. Normal macular thickness measurements in healthy eyes using Stratus optical coherence tomography. *Arch Ophthalmol*. 2006;124: 193–198.

16. Terry L, Cassels N, Lu K, et al. Automated retinal layer segmentation using spectral domain optical coherence tomography: evaluation of inter-session repeatability and agreement between devices. *PLoS One*. 2016;11:e0162001.

17. Chiu SJ, Izatt JA, O'Connell RV, Winter KP, Toth CA, Farsiu S. Validated automatic segmentation of AMD pathology including drusen and geographic atrophy in SD-OCT images. *Invest Ophthalmol Vis Sci*. 2012;53:53–61.

18. Ross DH, Clark ME, Godara P, et al. RefMoB, a reflectivity feature model-based automated method for measuring four outer retinal hyperreflective bands in optical coherence tomography. *Invest Ophthalmol Vis Sci*. 2015;56:4166–4176.

19. Staurenghi G, Sadda S, Chakravarthy U, Spaide RF; International Nomenclature for Optical Coherence Tomography Panel. Proposed lexicon for anatomic landmarks in normal posterior segment spectral-domain optical coherence tomography: the IN*OCT consensus. *Ophthalmology*. 2014;121: 1572–1578.

20. Stark K, Olden M, Brandl C, et al. The German AugUR study: study protocol of a prospective study to investigate chronic diseases in the elderly. *BMC Geriatr*. 2015;15:130.

21. Brandl C, Zimmermann ME, Gunther F, et al. On the impact of different approaches to classify age-related macular degeneration: Results from the German AugUR study. *Sci Rep*. 2018;8: 8675.

22. Abdolrahimzadeh S, Parisi F, Scavella V, Recupero SM. Optical coherence tomography evidence on the correlation of choroidal thickness and age with vascularized retinal layers in normal eyes. *Retina*. 2016;36:2329–2338.

23. Won JY, Kim SE, Park YH. Effect of age and sex on retinal layer thickness and volume in normal eyes. *Medicine (Baltimore)*. 2016;95:e5441.

24. Spaide RF, Curcio CA. Anatomical correlates to the bands seen in the outer retina by optical coherence tomography: literature review and model. *Retina*. 2011;31:1609–1619.

25. Kolb H. Simple anatomy of the retina. In: Kolb H, Fernandez E, Nelson R, eds., *Webvision: The Organization of the Retina and Visual System*. Salt Lake City, UT: University of Utah Health Sciences Center; 1995.

26. Klein R, Meuer SM, Myers CE, et al. Harmonizing the classification of age-related macular degeneration in the Three-Continent AMD Consortium. *Ophthalmic Epidemiol*. 2014;21:14–23.

27. Lei J, Balasubramanian S, Abdelfattah NS, Nittala MG, Sadda SR. Proposal of a simple optical coherence tomography-based scoring system for progression of age-related macular degeneration. *Graefes Arch Clin Exp Ophthalmol*. 2017; 255:1551–1558.

28. Spaide RF. Improving the age-related macular degeneration construct: a new classification system. *Retina*. 2018;38:891–899.

29. R Core Team. R: a language and environment for statistical computing. R Foundation for Statistical Computing, Vienna, Austria; 2017. Available from https://www.R-project.org/.

30. Bates D, Mächler M, Bolker B, Walker S. Fitting linear mixed-effects models using lme4. *J Stat Softw*. 2015;67:1–48.

31. Myers CE, Klein BE, Meuer SM, et al. Retinal thickness measured by spectral-domain optical coherence tomography in eyes without retinal abnormalities: the Beaver Dam Eye Study. *Am J Ophthalmol*. 2015;159:445–456.e441.

32. von Hanno T, Lade AC, Mathiesen EB, Peto T, Njolstad I, Bertelsen G. Macular thickness in healthy eyes of adults (N = 4508) and relation to sex, age and refraction: the Tromso Eye Study (2007-2008). *Acta Ophthalmol*. 2017;95:262–269.

33. Lee JY, Hwang YH, Lee SM, Kim YY. Age and retinal nerve fiber layer thickness measured by spectral domain optical coherence tomography. *Korean J Ophthalmol*. 2012;26:163–168.

34. Rougier MB, Korobelnik JF, Malet F, et al. Retinal nerve fibre layer thickness measured with SD-OCT in a population-based study of French elderly subjects: the Alienor study. *Acta Ophthalmol*. 2015;93:539–545.

35. Halekoh U, Højsgaard S. A Kenward-Roger approximation and parametric bootstrap methods for tests in linear mixed models - the R package pbkrtest. *J Stat Softw*. 2014;59:1–30.

36. Patel PJ, Foster PJ, Grossi CM, et al. Spectral-domain optical coherence tomography imaging in 67 321 adults: associations with macular thickness in the UK Biobank study. *Ophthalmology*. 2016;123:829–840.

37. Kashani AH, Zimmer-Galler IE, Shah SM, et al. Retinal thickness analysis by race, gender, and age using Stratus OCT. *Am J Ophthalmol*. 2010;149:496–502.e491.

38. Szigeti A, Tatrai E, Varga BE, et al. The effect of axial length on the thickness of intraretinal layers of the macula. *PLoS One*. 2015;10:e0142383.

39. Tan CS, Chan JC, Cheong KX, Ngo WK, Sadda SR. Comparison of retinal thicknesses measured using swept-source and spectral-domain optical coherence tomography devices. *Ophthalmic Surg Lasers Imaging Retina*. 2015;46:172–179.

40. Wang G, Qiu KL, Lu XH, Zhang MZ. Comparison and interchangeability of macular thickness measured with Cirrus OCT and Stratus OCT in myopic eyes. *Int J Ophthalmol*. 2015;8:1196–1201.

41. Brandao LM, Ledolter AA, Schotzau A, Palmowski-Wolfe AM. Comparison of two different OCT systems: retina layer segmentation and impact on structure-function analysis in glaucoma. *J Ophthalmol*. 2016;2016:8307639.

42. Curcio CA, Messinger JD, Sloan KR, Mitra A, McGwin G, Spaide RF. Human chorioretinal layer thicknesses measured in macula-wide, high-resolution histologic sections. *Invest Ophthalmol Vis Sci*. 2011;52:3943–3954.

43. Schuman SG, Koreishi AF, Farsiu S, Jung SH, Izatt JA, Toth CA. Photoreceptor layer thinning over drusen in eyes with age-related macular degeneration imaged in vivo with spectral-domain optical coherence tomography. *Ophthalmology*. 2009;116:488–496.e482.

44. Sadigh S, Cideciyan AV, Sumaroka A, et al. Abnormal thickening as well as thinning of the photoreceptor layer in intermediate age-related macular degeneration. *Invest Ophthalmol Vis Sci*. 2013;54:1603–1612.

45. Curcio CA, Medeiros NE, Millican CL. Photoreceptor loss in age-related macular degeneration. *Invest Ophthalmol Vis Sci*. 1996;37:1236–1249.

46. Owsley C, McGwin G Jr, Clark ME, et al. Delayed rod-mediated dark adaptation is a functional biomarker for incident early age-related macular degeneration. *Ophthalmology*. 2016;123:344–351.

47. Acton JH, Smith RT, Hood DC, Greenstein VC. Relationship between retinal layer thickness and the visual field in early age-related macular degeneration. *Invest Ophthalmol Vis Sci*. 2012;53:7618–7624.

48. Christenbury JG, Folgar FA, O'Connell RV, et al. Progression of intermediate age-related macular degeneration with prolifer-ation and inner retinal migration of hyperreflective foci. *Ophthalmology*. 2013;120:1038–1045.

49. Sevilla MB, McGwin G Jr, Lad EM, et al. Relating retinal morphology and function in aging and early to intermediate age-related macular degeneration subjects. *Am J Ophthalmol*. 2016;165:65–77.

50. Salmon AE, Sajdak BS, Atry F, Carroll J. Axial scaling is independent of ocular magnification in OCT images. *Invest Ophthalmol Vis Sci*. 2018;59:3037–3040.

51. Pan CW, Ikram MK, Cheung CY, et al. Refractive errors and age-related macular degeneration: a systematic review and meta-analysis. *Ophthalmology*. 2013;120:2058–2065.

52. Jonas JB, Xu L, Wei WB, et al. Retinal thickness and axial length. *Invest Ophthalmol Vis Sci*. 2016;57:1791–1797.

53. Carroll RJ, Ruppert D, Stefanski LA, Crainiceanu CM. Measurement error in nonlinear models: a modern perspec-tive. Chapter 15. Boca Raton, FL: CRC press; 2006.

54. Grace YY. Statistical analysis with measurement error or misclassification. Chapter 8.3. New York, NY: Springer New York. 2016.

55. Lujan BJ, Roorda A, Knighton RW, Carroll J. Revealing Henle's fiber layer using spectral domain optical coherence tomography. *Invest Ophthalmol Vis Sci*. 2011;52:1486–1492.

56. Lee DJ, Woertz EN, Visotcky A, et al. The Henle fiber layer in albinism: comparison to normal and relationship to outer nuclear layer thickness and foveal cone density. *Invest Ophthalmol Vis Sci*. 2018;59:5336–5348.